

# Photocatalytic CO<sub>2</sub> Reduction to Produce Cleaner Fuels Over Vanadium Aluminium Carbide (V<sub>2</sub>AlC) Supported TiO<sub>2</sub> Composite

Muhammad Tahir

Chemical and Petroleum Engineering Department, College of Engineering, UAE University, P.O. Box 15551, United Arab Emirates.

[muhammad.tahir@uaeu.ac.ae](mailto:muhammad.tahir@uaeu.ac.ae)

Photocatalytic reduction of CO<sub>2</sub> to produce cleaner fuels is a promising approach for climate action to achieve sustainable development goals. Herein, noble metal-free vanadium aluminium carbide (V<sub>2</sub>AlC) MAX as cocatalysts with TiO<sub>2</sub> to construct 2D/0D V<sub>2</sub>AlC/TiO<sub>2</sub> heterojunction for photocatalytic CO<sub>2</sub> reduction with water to produce CO and CH<sub>4</sub> has been investigated. Coupling V<sub>2</sub>AlC with TiO<sub>2</sub> was beneficial in increasing visible light absorbance capacity and charge separation efficiency. Using 10 % V<sub>2</sub>AlC/TiO<sub>2</sub> composite, the highest CO and CH<sub>4</sub> production of 522 and 78.3 μmol g<sup>-1</sup> h<sup>-1</sup> were achieved, which were much higher than using pristine TiO<sub>2</sub> samples. This significant enhancement in photocatalytic efficiency was due to good interface interaction with proficient charge carrier separation. The findings of this work would be beneficial for further investigation in the design and fabrication of noble metal-free composite materials for energy and environmental applications.

## 1. Introduction

Photocatalytic CO<sub>2</sub> reduction using a semiconductor and energy source (light) produces various chemicals and fuels such as methane, methanol, carbon monoxide, acetic acid, and formic acid. For these processes, various photocatalysts including TiO<sub>2</sub>, CdS, ZnO, and WO<sub>3</sub> were explored. Due to its low-cost, strong photostability, and suitable redox potential, TiO<sub>2</sub> is one of the most extensively researched semiconductors (Wang et al., 2023). TiO<sub>2</sub> has a number of advantages, however, its photoactivity and selectivity are reduced because of charge carrier recombination (Ren et al., 2023). As a result, TiO<sub>2</sub> photoactivity can be enhanced by loading with metals and using low-cost materials to develop TiO<sub>2</sub>-based composites (Beenish et al., 2018).

MAX materials with the general formula M<sub>n+1</sub>AX<sub>n</sub>, are made of three elements, transition metals (M element), elements of group III or IV (A element) and either C or N elements (X element), which have layered structures and compact sheets. Multiple researchers have become interested in them due to their numerous distinctive qualities, including strong conductivity, charge carrier transfer ability, inexpensive cost, and improved stability (Bai et al., 2022). In the past, titanium aluminium carbide (Ti<sub>3</sub>AlC<sub>2</sub>) MAX was put to the test in photocatalytic applications and found to be effective in reducing CO<sub>2</sub> levels. Another significant MAX that is based on multiple oxidation states is V<sub>2</sub>AlC because vanadium possesses several oxidation states. This MAX has various distinguishing qualities, including a greater capacity to absorb visible light, superior electrical conductivity, and chemical and thermal stability (Presser et al., 2012). Previous V<sub>2</sub>AlC/g-C<sub>3</sub>N<sub>4</sub> was invested for photocatalytic water splitting, and higher hydrogen production was achieved (Tahir et al., 2021). As a result, V<sub>2</sub>AlC can be further investigated for use as a photocatalyst and producing a V<sub>2</sub>AlC/TiO<sub>2</sub> heterojunction would improve the effectiveness of CO<sub>2</sub> reduction to yield useful chemicals and fuels.

In this work, V<sub>2</sub>AlC supported TiO<sub>2</sub> composite for photocatalytic CO<sub>2</sub> reduction in a fixed bed photoreactor has been investigated. The composites were synthesized using a facile sol-gel single step method to get good interface interaction between both the materials. The composites were analyzed using XRD, UV, visible, SEM, and PL characterization techniques. The composite found promising for selective CO<sub>2</sub> reduction to cleaner fuels with higher efficiency. The reaction mechanism was proposed based on findings of characterization and experimental results.

## 2. Experimental

### 2.1 Catalyst Synthesis

V<sub>2</sub>AlC/TiO<sub>2</sub> composite was synthesized using the sol-gel method. Titanium sol was obtained by hydrolyzing TTIP (Titanium (IV) isopropoxide (Sigma Aldrich)) in acetic acid (1 M) using 10 mL of TTIP that was dissolved in 2-propanol, in accordance with a procedure reported previously (Tahir 2020). Typically, specific amount of V<sub>2</sub>AlC MAX (10 weight %) dispersed in 2-propanol was added to the titanium solution after stirring for 4 h. The suspension was then stirred for 24 h before being overnight oven dried at 100 °C. The final product was ground before being calcined at 500 °C for two hours and was given name V<sub>2</sub>AlC/TiO<sub>2</sub> composite.

### 2.2 Catalyst Characterization

The purity and crystal phase structures were studied using X-ray powder diffraction (XRD) on a Bruker Advance D8 diffractometer (Rigaku Smart Lab-Cu-K,  $\lambda=0.154178$  nm). The morphology was obtained using scanning electron microscopy (SEM, JEOL 6010 PLUS/LA). Using a 325 nm laser, photoluminescence (PL) spectroscopy was carried out (HORIBA Scientific) to measure the charges separation efficiency in the composite material. The UV-visible diffuse reflectance absorbance spectra were obtained using Carry 100 Agilent UV-vis spectrophotometer (model # G9821A).

### 2.3 Photoactivity test

The photocatalytic CO<sub>2</sub> reduction experiments were conducted using fixed bed photoreactor system. The primary reactor chamber, cooling fans integrated with lamps, mass flow controllers (MFC), and an online system for product analysis are all parts of the photocatalytic system. A water saturator was combined with the reactor system, in which CO<sub>2</sub> was passed to carry water vapours. A 150 mg photocatalysts was dispersed in the reactor bottom surface. The feed mixture entered the reactor from the top, passed over the catalyst surface, and then exited the reactor from the bottom surface. A feed combination (CO<sub>2</sub> and H<sub>2</sub>O) was constantly fed into the reactor at 20 mL/min for 30 min prior to the experimentation to saturate the catalyst surface. The gas products were analyzed using GC which was integrated with TCD and FID detectors. After regular intervals of 30 min, samples were injected into GC using a gas-tight syringe and production of CO and CH<sub>4</sub> was calculated using GC results. All the experiments were conducted at normal temperature and atmospheric pressure.

## 3. Results and discussion

### 3.1 Materials analysis

Figure 1 (a) shows XRD patterns of TiO<sub>2</sub>, V<sub>2</sub>AlC and V<sub>2</sub>AlC/TiO<sub>2</sub> composite samples. The XRD spectra of V<sub>2</sub>AlC MAX shows two main peaks with 2-theta of 13.46° and 41.16° associated to (0 0 2) and (1 0 3) facets of V<sub>2</sub>AlC MAX, and similarly reported previously in the literature (Madi et al., 2022). The XRD of TiO<sub>2</sub> confirms successful synthesis of anatase phase and was in accordance with JCPDS Card No. 01-084-1285. In V<sub>2</sub>AlC/TiO<sub>2</sub> composite, all the original peaks were appeared, which confirm successful synthesis.

The UV-visible analysis of TiO<sub>2</sub> and V<sub>2</sub>AlC/TiO<sub>2</sub> composite has been demonstrated in Figure 1 (b). TiO<sub>2</sub> was used to measure light absorption in the UV-visible range with a band edge just below 400 nm. The band edge was shifted to the visible light region, above 400 nm, when V<sub>2</sub>AlC was coupled with TiO<sub>2</sub> to produce V<sub>2</sub>AlC/TiO<sub>2</sub> composite with greater visible light absorbance. This is because pure V<sub>2</sub>AlC MAX demonstrates higher visible spectrum light absorption because of its dark hue and conductive properties (Zhao et al., 2022). The band gap energies were estimated for pure TiO<sub>2</sub> and V<sub>2</sub>AlC/TiO<sub>2</sub> composites were 3.40 and 2.96 eV. Previously, the energy of the band gap increased from 3.14 to 3.22 eV when Ti<sub>3</sub>AlC<sub>2</sub> was added to TiO<sub>2</sub> (Tahir et al., 2022). All of these findings show that V<sub>2</sub>AlC has features of visible light absorption and significantly lowers the band gap energy of TiO<sub>2</sub>.

Figure 1 (c) discusses the findings of charges separation of TiO<sub>2</sub> and V<sub>2</sub>Al/TiO<sub>2</sub> through photoluminescence (PL) analysis. Because charge recombination occurs at a faster rate in pure TiO<sub>2</sub>, it is evident that it has the highest PL intensity. Loading V<sub>2</sub>AlC into TiO<sub>2</sub>, PL intensity was significantly decreased. This is because, MAX has greater ability to conduct electrons what keeps charges from recombining in the V<sub>2</sub>AlC/TiO<sub>2</sub> composite, lowering the PL intensity noticeably. In a recent study, V<sub>2</sub>C MXene and g-C<sub>3</sub>N<sub>4</sub> were coupled and the PL intensity was significantly reduced as a result of effective charge carrier separation (Tahir, 2023).

Figure 2 shows the morphology of TiO<sub>2</sub>, V<sub>2</sub>AlC and V<sub>2</sub>AlC/TiO<sub>2</sub> composites. The morphology of TiO<sub>2</sub> is depicted in Figure 2(a), where spherical-shaped particles of uniform size can be seen. The morphology of V<sub>2</sub>AlC/TiO<sub>2</sub> composite is depicted in Figure 2(b-c). To give their strong interface interaction, TiO<sub>2</sub> particles are evenly dispersed throughout the V<sub>2</sub>AlC structure. Further research revealed that the constant stirring during the sol-gel process in the presence of alcohols caused the bulk structure of V<sub>2</sub>AlC to exfoliate. V<sub>2</sub>AlC sheets were

completely covered with  $\text{TiO}_2$  particles, providing good interaction that would be useful to transport charges. Figure 2 (d) shows EDX spectra of  $\text{V}_2\text{AlC}/\text{TiO}_2$  composite, in which all the elements are present.

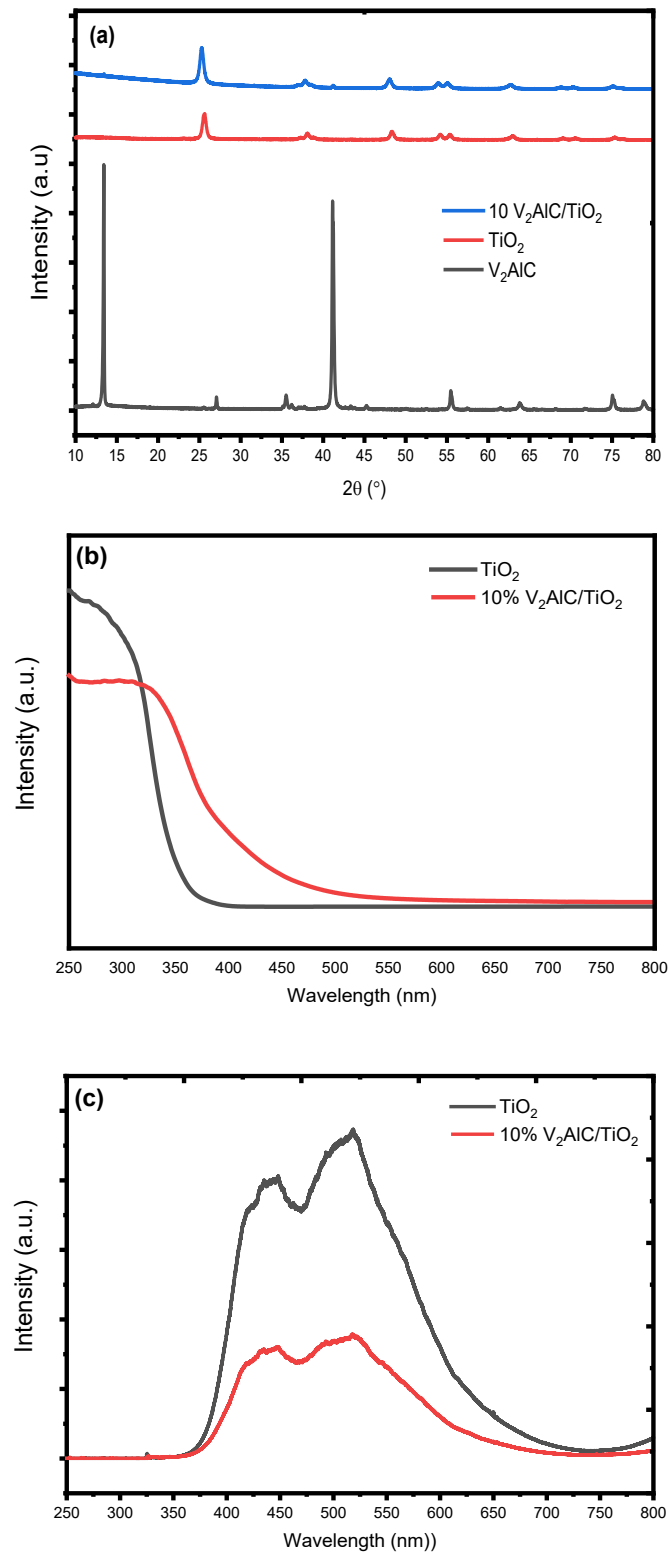


Figure 1: (a) XRD patterns of  $\text{TiO}_2$  and  $\text{V}_2\text{AlC}/\text{TiO}_2$ , (b) UV-visible diffuse reflectance spectra of  $\text{TiO}_2$  and  $\text{V}_2\text{AlC}/\text{TiO}_2$  and (c) PL analysis of  $\text{TiO}_2$  and  $\text{V}_2\text{AlC}/\text{TiO}_2$  samples.

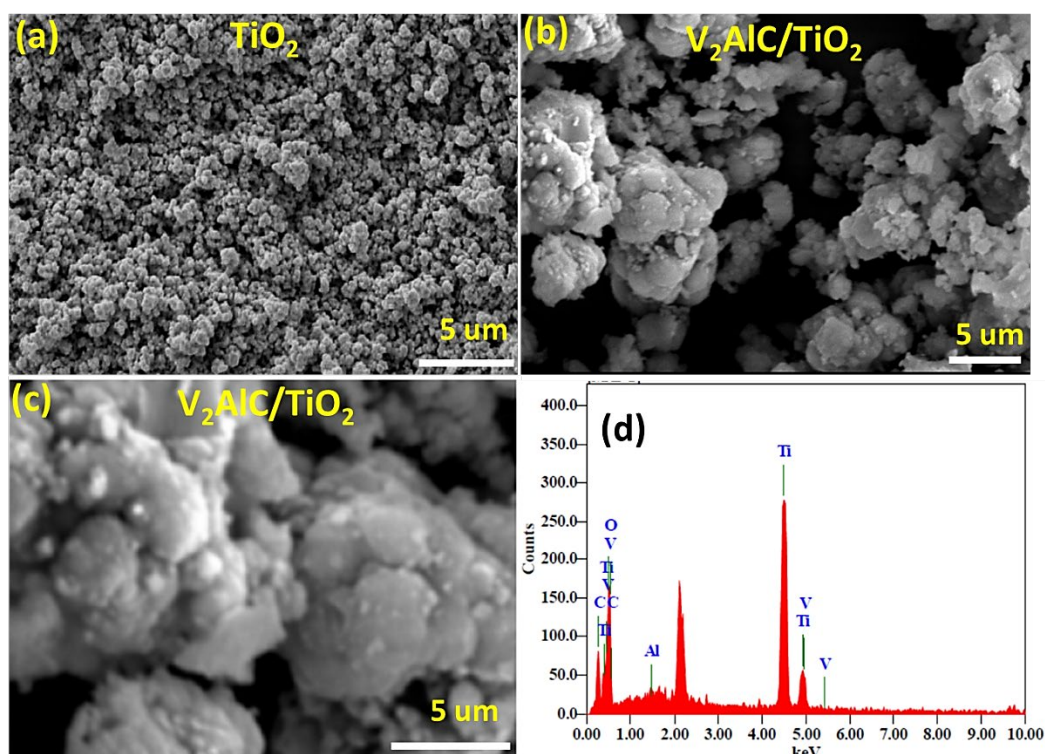


Figure 2: SEM analysis of (a)  $\text{TiO}_2$ , (b-c)  $\text{V}_2\text{AlC}/\text{TiO}_2$ , (d) EDX plot of  $\text{V}_2\text{AlC}/\text{TiO}_2$  composite.

### 3.2 Photocatalytic hydrogen production

Blank experiments were first carried out to make sure that all of the products were produced only from the  $\text{CO}_2$  and not from organic residues in the composite photocatalyst. These quality control tests show that the photocatalyst or feed mixture, both of which are necessary for any photocatalysis process, were not used to produce the products. The performance of  $\text{TiO}_2$  and  $\text{V}_2\text{AlC}/\text{TiO}_2$  composite for photocatalytic  $\text{CO}_2$  reduction to  $\text{CO}$  and  $\text{CH}_4$  is shown in Figure 3.

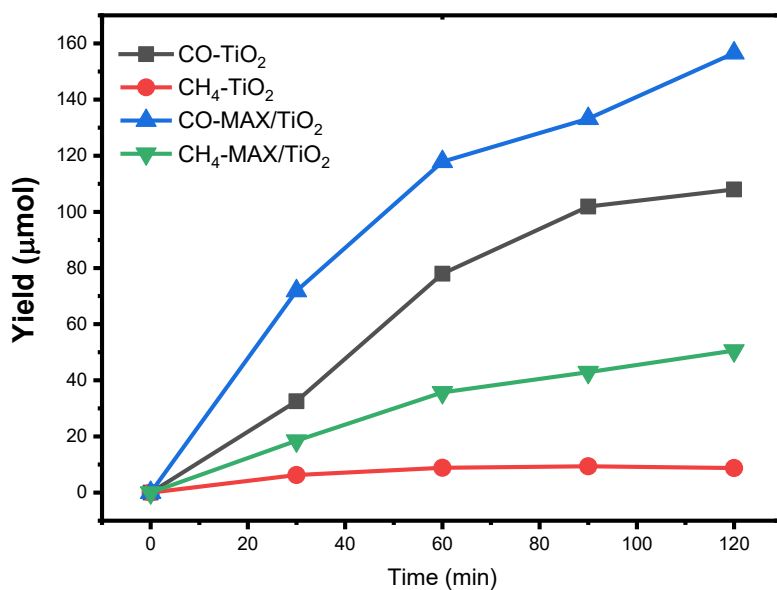


Figure 3: Performance comparison of  $\text{TiO}_2$  and  $\text{V}_2\text{AlC}$ -loaded  $\text{TiO}_2$  for photocatalytic  $\text{CO}_2$  reduction to  $\text{CO}$  and  $\text{CH}_4$  in a fixed bed reactor.

Using both the materials, CO was identified as the main product with lower amount of CH<sub>4</sub> formation. Obviously, production of CO and CH<sub>4</sub> was continuous over the entire irradiation time. Using pure TiO<sub>2</sub>, lower amount of CO (108 μmol) and CH<sub>4</sub> (8.76 μmol) were produced, which were due to charge carrier recombination. When 10 % V<sub>2</sub>AIC was loaded with TiO<sub>2</sub>, CO and CH<sub>4</sub> production was increased to 156.53 and 50.6 μmol, respectively was achieved. Typically, production of CH<sub>4</sub> increment was much higher compared to CO, which was evidently due to more production and separation of photoinduced charge carrier. V<sub>2</sub>AIC has potential to increase light absorbance and preventing the recombination of charges, which was beneficial to promote photocatalytic efficiency.

Numerous studies that are currently available discuss the use of TiO<sub>2</sub> based photocatalyst for photocatalytic CO<sub>2</sub> reduction to CO and CH<sub>4</sub> under UV and visible light irradiations. The photocatalytic activity for the selective reduction of CO<sub>2</sub> was shown to be improved in prior studies using 2D Ti<sub>3</sub>AlC<sub>2</sub> MAX supported TiO<sub>2</sub> (Tahir 2020). Similar to this, when the photocatalytic CO<sub>2</sub> reduction were investigated using V<sub>2</sub>AIC loaded g-C<sub>3</sub>N<sub>4</sub> composite, the production of CO was greatly increased due to effective charge carrier separation (Tahir et al., 2022). In a different experiment, g-C<sub>3</sub>N<sub>4</sub>-loaded Ti<sub>3</sub>C<sub>2</sub> was more effectively able to reduce CO<sub>2</sub> to CH<sub>4</sub> with high selectivity. In addition to improved light-harvesting ability, the greatly increased photoactivity was caused by improved CO<sub>2</sub> adsorption/activation (Hu et al., 2021). The performance of V<sub>2</sub>AIC/TiO<sub>2</sub> for photocatalytic CO<sub>2</sub> reduction in view of production rate and selectivity are summarized in Table 1. Using TiO<sub>2</sub> and V<sub>2</sub>AIC/TiO<sub>2</sub>, CO was obtained as the main product during photocatalytic CO<sub>2</sub> reduction with H<sub>2</sub>O. The highest CO and CH<sub>4</sub> production rates of 522 and 78.3 μmol g<sup>-1</sup> h<sup>-1</sup>, which was 1.45 and 2.68 folds higher for CO and CH<sub>4</sub> production than using pure TiO<sub>2</sub> samples. Similar to this, CO and CH<sub>4</sub> selectivity of 92.5 and 7.5 % over TiO<sub>2</sub>, which was changes to 86.96 and 13.04 % when V<sub>2</sub>AIC was coupled with TiO<sub>2</sub>. This increase in CH<sub>4</sub> selectivity was due to more production and separation over V<sub>2</sub>AIC/TiO<sub>2</sub> composite. Figure 4 shows photocatalytic CO<sub>2</sub> reduction over a V<sub>2</sub>AIC/TiO<sub>2</sub> composite for the production of CO, and CH<sub>4</sub>. The photogenerated charges on the TiO<sub>2</sub> under light irradiation can combine again because of their short life time. However, effective photoinduced charge separation was achieved by creating a heterojunction between V<sub>2</sub>AIC and TiO<sub>2</sub> (Majhi et al., 2023). The holes were used for water oxidation, whereas, electrons were used for CO<sub>2</sub> reduction to CO and CH<sub>4</sub>. Due to the increased electrical conductivity of MAX-based materials, higher separation of charges with their lowest recombination over TiO<sub>2</sub> can be achieved. The generation of CO was significantly higher than that of CH<sub>4</sub> because of the favourable reaction due to involving only two electrons, compared to eight electrons for CH<sub>4</sub> formation. Using V<sub>2</sub>AIC/TiO<sub>2</sub> composite, production was CH<sub>4</sub> was higher due to more production and separation of charge carriers.

Table 1: Summary of yield rate and selectivity for CO and CH<sub>4</sub> production over TiO<sub>2</sub> and 10 % V<sub>2</sub>AIC/TiO<sub>2</sub> composite in a fixed bed photoreactor

Catalyst	Production rate (μmol g <sup>-1</sup> h <sup>-1</sup> )		Selectivity (%)	
	CO	CH <sub>4</sub>	CO	CH <sub>4</sub>
TiO <sub>2</sub>	360	29.2	92.50	7.50
10 % V <sub>2</sub> AIC/TiO <sub>2</sub>	522	78.3	86.96	13.04

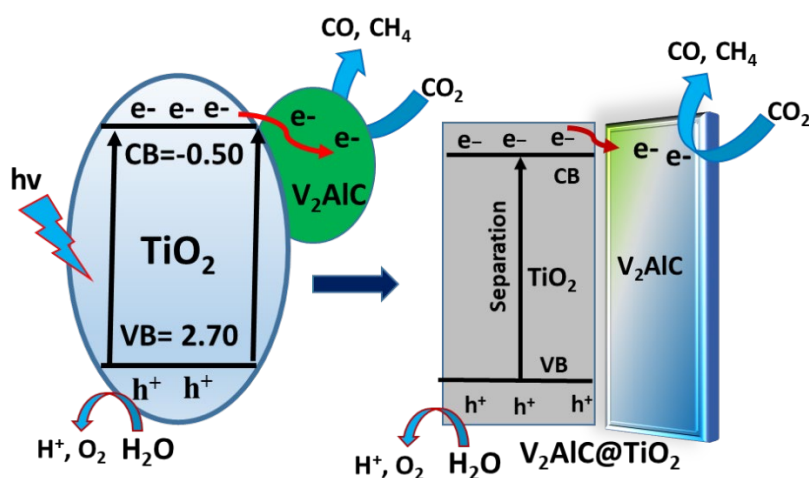


Figure 4: Schematic presentation of the proposed mechanism of V<sub>2</sub>AIC/TiO<sub>2</sub> composite for photocatalytic CO<sub>2</sub> reduction to CO and CH<sub>4</sub> under UV-light irradiation.

#### 4. Conclusions

The  $V_2AlC$  loaded  $TiO_2$  composite was successfully synthesized using sol-gel single step method. Higher light absorption and effective charge carrier separation during the photocatalytic process were responsible for increasing photocatalytic  $CO_2$  reduction efficiency over  $V_2AlC/TiO_2$  composite.  $CO$  and  $CH_4$  were produced as the main products during  $CO_2$  reduction with water in a fixed bed photoreactor. The  $CO$  was produced at a significantly higher rate compared to methane due to using  $TiO_2$  as a catalyst, which is supportive to produce more  $CO$ . When  $V_2AlC$  was coupled with  $TiO_2$ , production of  $CH_4$  was increased. It can be concluded that to increase photocatalytic efficiency,  $V_2AlC$  MAX can be utilized directly as a cocatalyst with semiconductor materials rather than being converted into MXene using hazardous acids. The results of this research offer hope for developing more effective, structured photocatalytic systems that can be applied to both energy and environmental applications.

#### Acknowledgments

United Arab Emirates University (UAEU) provided funding for this work through a SURE PLUS grant (Grant # G00004006).

#### References

- Bai J., Chen W., Shen R., Jiang Z., Zhang P., Liu W., Li X., 2022, Regulating interfacial morphology and charge-carrier utilization of  $Ti_3C_2$  modified all-sulfide  $CdS/ZnIn_2S_4$  S-scheme heterojunctions for effective photocatalytic  $H_2$  evolution, *Journal of Materials Science & Technology* 112, 85-95.
- Beenish T., Tahir M., and Amin N.A.S., 2018, Photocatalytic  $CO_2$ -Hydrogen Conversion via RWGS over  $Ni/TiO_2$  Nanocatalyst Dispersed in Layered MMT Nanoclay, *Chemical Engineering Transactions* 63, 115-120.
- Hu J., Ding J., Zhong Q., 2021, Ultrathin 2D  $Ti_3C_2$  MXene Co-catalyst anchored on porous  $g-C_3N_4$  for enhanced photocatalytic  $CO_2$  reduction under visible-light irradiation, *Journal of Colloid and Interface Science* 582(Pt B), 647-657.
- Madi M., Tahir M., 2022, Fabricating  $V_2AlC/g-C_3N_4$  nanocomposite with MAX as electron moderator for promoting photocatalytic  $CO_2$ - $CH_4$  reforming to  $CO/H_2$ , *International Journal of Energy Research*, 7666-7685.
- Majhi S.M., Ali A., Greish Y.E., El-Maghraby H.F., Mahmoud S.T., 2023,  $V_2CT_x$  MXene-based hybrid sensor with high selectivity and ppb-level detection for acetone at room temperature, *Scientific Reports* 13(1), 3114.
- Presser V., Naguib M., Chaput L., Togo A., Hug G., Barsoum M.W., 2012, First-order Raman scattering of the MAX phases:  $Ti_2AlN$ ,  $Ti_2AlC_{0.5}N_{0.5}$ ,  $Ti_2AlC$ ,  $(Ti_{0.5}V_{0.5})_2AlC$ ,  $V_2AlC$ ,  $Ti_3AlC_2$ , and  $Ti_3GeC_2$ , *Journal of Raman Spectroscopy*, 43 (1), 168-172.
- Ren G., Wei Z., Li Z., Zhang X., Meng X., 2023, Fabrication of S-scheme hollow  $TiO_2@Bi_2MoO_6$  composite for efficiently photocatalytic  $CO_2$  reduction, *Materials Today Chemistry*, 27, 101260.
- Tahir B., Tahir M., Nawawi M.G.M., 2022, Highly stable honeycomb structured 2D/2D vanadium aluminum carbide MAX coupled  $g-C_3N_4$  composite for stimulating photocatalytic  $CO_2$  reduction to  $CO$  and  $CH_4$  in a monolith photoreactor, *Journal of Alloys and Compounds* 927, 166908.
- Tahir M., 2020, Enhanced photocatalytic  $CO_2$  reduction to fuels through bireforming of methane over structured 3D MAX  $Ti_3AlC_2/TiO_2$  heterojunction in a monolith photoreactor, *Journal of  $CO_2$  Utilization* 38, 99-112.
- Tahir M., 2023, Vanadium Carbide ( $V_2CT_x$ ) MXene-Supported Exfoliated  $g-C_3N_4$  with the Role of Hole Scavenger as a Rapid Electron Transfer Channel for Enhancing Photocatalytic  $CO_2$  Reduction to  $CO$  and  $CH_4$ , *Energy & Fuels* 37(14), 10615-10630.
- Wang Y., He W., Xiong J., Tang Z., Wei Y., Wang X., Xu H., Zhang X., Zhao Z., Liu J., 2023, MIL-68 (In)-derived  $In_2O_3@TiO_2$  S-scheme heterojunction with hierarchical hollow structure for selective photoconversion of  $CO_2$  to hydrocarbon fuels, *Fuel* 331.
- Zhao R., Liu J., Nie Y., Wang H., 2022, Bismuth oxide modified  $V_2C$  MXene as a Schottky catalyst with enhanced photocatalytic oxidation for photo-denitration activities, *Environmental Technologies*, 1-12.